Proc. Natl. Acad. Sci. USA
Vol. 92, pp. 7242–7246, August 1995
Neurobiology

In vitro autoradiography of receptor-activated G proteins in rat brain by agonist-stimulated guanylyl 5′-[γ-[^{35}S]thio]-triphosphate binding

(opioid receptor/cannabinoid receptor/γ-aminobutyric acid type B receptor)

LAURA J. SIM, DANA E. SELLEY, AND STEVEN R. CHILDERS*

Department of Physiology and Pharmacology, Bowman Gray School of Medicine, Wake Forest University, Medical Center Boulevard, Winston-Salem, NC 27157

Communicated by Louis Sokoloff, National Institute of Mental Health, Bethesda, MD, April 11, 1995 (received for review February 15, 1995)

ABSTRACT **Agonists stimulate guanylyl 5′-[γ-[^{35}S]thio]-triphosphate (GTP[γ-^{35}S]) binding to receptor-coupled guanine nucleotide binding protein (G proteins) in cell membranes as revealed in the presence of excess GDP. We now report that this reaction can be used to neuroanatomically localize receptor-activated G proteins in brain sections by *in vitro* autoradiography of GTP[γ-^{35}S] binding. Using the μ opioid-selective peptide [D-Ala^2,*N*-MePhe^4,Gly^5-ol]enkephalin (DAMGO) as an agonist in rat brain sections and isolated thalamic membranes, agonist stimulation of GTP[γ-^{35}S] binding required the presence of excess GDP (1–2 mM GDP in sections vs. 10–30 μM GDP in membranes) to decrease basal G-protein activity and reveal agonist-stimulated GTP[γ-^{35}S] binding. Similar concentrations of DAMGO were required to stimulate GTP[γ-^{35}S] binding in sections and membranes. To demonstrate the general applicability of the technique, agonist-stimulated GTP[γ-^{35}S] binding in tissue sections was assessed with agonists for the μ opioid (DAMGO), cannabinoid (WIN 55212-2), and γ-aminobutyric acid type B (baclofen) receptors. For opioid and cannabinoid receptors, agonist stimulation of GTP[γ-^{35}S] binding was blocked by incubation with agonists in the presence of the appropriate antagonists (naloxone for μ opioid and SR-141716A for cannabinoid), thus demonstrating that the effect was specifically receptor mediated. The anatomical distribution of agonist-stimulated GTP[γ-^{35}S] binding qualitatively paralleled receptor distribution as determined by receptor binding autoradiography. However, quantitative differences suggest that variations in coupling efficiency may exist between different receptors in various brain regions. This technique provides a method of functional neuroanatomy that identifies changes in the activation of G proteins by specific receptors.**

Guanine nucleotide binding protein (G protein)-coupled receptors comprise the majority of receptor types in the central nervous system, since at least 80% of all known intercellular signaling factors (neurotransmitters, hormones, etc.) produce biological responses by binding to and activating receptors that are G-protein coupled (1). A variety of intracellular effectors are controlled by G proteins, including the activity of adenylyl cyclase, phosphodiesterases, phospholipases A and C, and calcium and potassium channel conductance (1–5). These effectors in turn regulate neuronal activity and modulate the expression of a variety of genes (6–8). Previous biochemical studies of G-protein-coupled receptors have allowed examination of the cascade at the level of the receptor, G protein, and effectors (1, 4, 5). However, anatomical studies have been limited to immunocytochemical localization of G proteins (9–11) and *in situ* hybridization (12–14) or autoradiography (15–19) of receptor binding sites. Guanine nucleotides have been shown to inhibit agonist binding to G-protein-coupled receptors as measured autoradiographically in tissue sections (20), suggesting that receptor–G-protein complexes remain functional in tissue sections. Although these techniques have been useful for localizing receptors and G proteins, and studying receptor binding properties, no anatomical technique has been available to directly measure the functional activity of receptor-mediated events. In particular, measurements of receptor binding sites in neural membranes do not necessarily correlate with functional coupling to intracellular signal transduction mechanisms (21). Moreover, numerous examples of mismatch exist between the neuroanatomical distribution of receptor binding sites and their corresponding neurotransmitters (22).

Receptor-stimulated guanylyl 5′-[γ-[^{35}S]thio]triphosphate (GTP[γ-^{35}S]) binding has been used in biochemical studies of purified and reconstituted systems to measure receptor activation of G proteins (23, 24). More recently, this technique has been used in isolated membranes to measure the activation of G proteins by specific receptors (25, 26). These results demonstrated that significant agonist stimulation of GTP[γ-^{35}S] binding occurred in membranes only in the presence of relatively large concentrations (3–10 μM) of GDP. Such concentrations of GDP were necessary to inactivate G proteins, so that stimulation of GTP[γ-^{35}S] binding over basal levels could be observed when agonists were added to membrane preparations. We now report the development of an *in vitro* anatomical technique by which receptor-activated G proteins can be identified autoradiographically by using GTP[γ-^{35}S] binding to tissue sections. The present study compares the autoradiographic distribution of GTP[γ-^{35}S] binding after stimulation by agonists for three different receptors, which numerous studies have identified as typical members of the G-protein-coupled receptor superfamily: μ opioid (27), cannabinoid (28), and type B γ-aminobutyric acid receptor ($GABA_B$) (29).

MATERIALS AND METHODS

Materials. Sprague–Dawley rats were obtained from Zivic–Miller. GTP[γ-^{35}S] (1393 Ci/mmol; 1 Ci = 37 GBq) was purchased from New England Nuclear. Hyperfilm-βmax film was purchased from Amersham. [D-Ala^2,*N*-MePhe^4,Gly^5-ol]enkephalin (DAMGO) and naloxone were purchased from Sigma. Baclofen was obtained from Research Biochemicals International (Natick, MA). WIN 55212-2 was a kind gift from S. Ward, Sterling Research Group. SR141716A was a kind gift from F. Barth (Sanofi, Paris). GDP and GTP[γS] were purchased from Boehringer Mannheim. All other reagent grade chemicals were obtained from Sigma or Fisher.

The publication costs of this article were defrayed in part by page charge payment. This article must therefore be hereby marked "*advertisement*" in accordance with 18 U.S.C. §1734 solely to indicate this fact.

Abbreviations: DAMGO, [D-Ala^2,*N*-MePhe^4,Gly^5-ol]enkephalin; GTP[γ-^{35}S], guanylyl 5′-[γ-^{35}S]thio]triphosphate; G protein, guanine nucleotide binding protein; $GABA_B$, type B γ-aminobutyric acid receptor.

*To whom reprint requests should be addressed.

Agonist-Stimulated GTP[γ-^{35}S] Binding Autoradiography. Male Sprague–Dawley rats (150–200 g) were sacrificed by decapitation. The brains were removed and immediately immersed in isopentane at −35°C. Coronal or horizontal sections (20 μm) were cut on a cryostat at −20°C and thaw-mounted onto gelatin-coated slides. Slides were dried under a vacuum and stored desiccated at −80°C until use. Slides were incubated in assay buffer (50 mM Tris·HCl/3 mM $MgCl_2$/0.2 mM EGTA/100 mM NaCl, pH 7.7) at 25°C for 10 min. Slides were then incubated with the appropriate concentration of GDP in assay buffer at 25°C for 15 min. Agonist-stimulated activity was determined by incubating in GTP[γ-^{35}S] (0.04 nM) with the appropriate agonist and GDP concentrations in assay buffer at 25°C for 2 hr. The incubation medium for WIN 55212-2 also contained 0.5% bovine serum albumin. Agonist studies were also performed in the presence of appropriate antagonists to verify the receptor specificity of G-protein activation. In each experiment, basal activity was assessed with GDP in the absence of agonist, and nonspecific binding was assessed in the presence of 10 μM unlabeled GTP[γS] without GDP. Slides were then rinsed twice in ice-cold Tris buffer (50 mM Tris·HCl, pH 7.0 at 25°C) and rinsed once briefly in deionized water. Slides were dried overnight and exposed to Hyperfilm-βmax for 24 hr. Films were digitized with a Sony XC-77 video camera and analyzed using the National Institutes of Health IMAGE program for Macintosh computers. Quantification of images was obtained from densitometric analysis using ^{14}C standards. Agonist-stimulated activity in brain sections was calculated by subtracting the optical density in basal sections (incubated with GDP alone) from that of agonist-stimulated sections; results were expressed as percentage basal activity. All autoradiograms shown represent typical sections, which were performed in duplicate and repeated at least three times. In some experiments, labeled sections were stripped from slides and ^{35}S radioactivity was determined by liquid scintillation spectrophotometry.

Agonist-Stimulated GTP[γ-^{35}S] Binding in Membranes. Rats were sacrificed by decapitation; the thalamus was dissected and homogenized in 20 vol of ice-cold Tris·Mg^{2+} buffer (50 mM Tris·HCl/3 mM $MgCl_2$/1 mM EGTA, pH 7.4) with a Polytron (Brinkmann). The homogenate was centrifuged at 48,000 × g at 4°C for 10 min, resuspended in assay buffer, centrifuged again at 48,000 × g at 4°C for 10 min, and finally resuspended in assay buffer. Protein levels were determined by the method of Bradford (30). Membranes (10 μg of protein) were incubated at 30°C for 1 hr in assay buffer with the appropriate concentrations of DAMGO and/or GDP in the presence of 0.05 nM GTP[γ-^{35}S] in 1 ml total volume. Basal binding was assessed in the absence of agonist and presence of GDP, and nonspecific binding was assessed in the presence of 10 μM unlabeled GTP[γS]. The reaction was terminated by rapid filtration under vacuum through Whatman GF/B glass fiber filters, followed by three washes with 3 ml of ice-cold Tris buffer. Bound radioactivity was determined by liquid scintillation spectrophotometry at 95% efficiency after extraction overnight in 5 ml of Ecolite scintillation fluid (ICN). Data are reported as means ± SE values of at least three experiments, which were each performed in triplicate. Nonlinear iterative regression analyses of agonist concentration–effect curves were performed with JMP (SAS Institute, Cary, NC). The resulting ED_{50} values were used to determine K_e values for antagonism of the agonist-stimulated response by naloxone, using the relationship $K_e = [Ant]/(DR - 1)$, where [Ant] is the concentration of antagonist, and DR is the ratio of ED_{50} values in the presence and absence of antagonist.

RESULTS

Previous studies in isolated membranes have shown that agonists of G-protein-coupled receptors produce significant stimulation of GTP[γ-^{35}S] binding when assays were performed in the presence of a large excess of GDP in order to ensure that G proteins were present in the inactivated state (25, 26). To determine the conditions required for detecting agonist stimulation of GTP[γ-^{35}S] binding by autoradiography of brain sections, agonist-stimulated GTP[γ-^{35}S] binding was compared between rat brain sections (cut at the level of the thalamus) and isolated thalamic membranes using the μ opioid agonist DAMGO. The appropriate concentrations of GDP for detecting agonist-stimulated GTP[γ-^{35}S] binding were determined in tissue sections and thalamic membranes by incubating with various concentrations of GDP with and without DAMGO (Fig. 1). In thalamic membranes, GDP (1–100 μM) inhibited GTP[γ-^{35}S] binding in a concentration-dependent manner, with <3% of total GTP[γ-^{35}S] bound with 100 μM GDP (Fig. 1 *Left*). DAMGO produced little significant effect on binding in the absence of GDP, and relative stimulation by the agonist increased with increasing concentrations of GDP. This effect is best observed in Fig. 1 (*Inset*), which shows that the relative percentage stimulation by DAMGO increased as the concentration of GDP was increased, with significant stimulation obtained at GDP concentrations over 1 μM. In tissue sections, GTP[γ-^{35}S] binding was more resistant to the

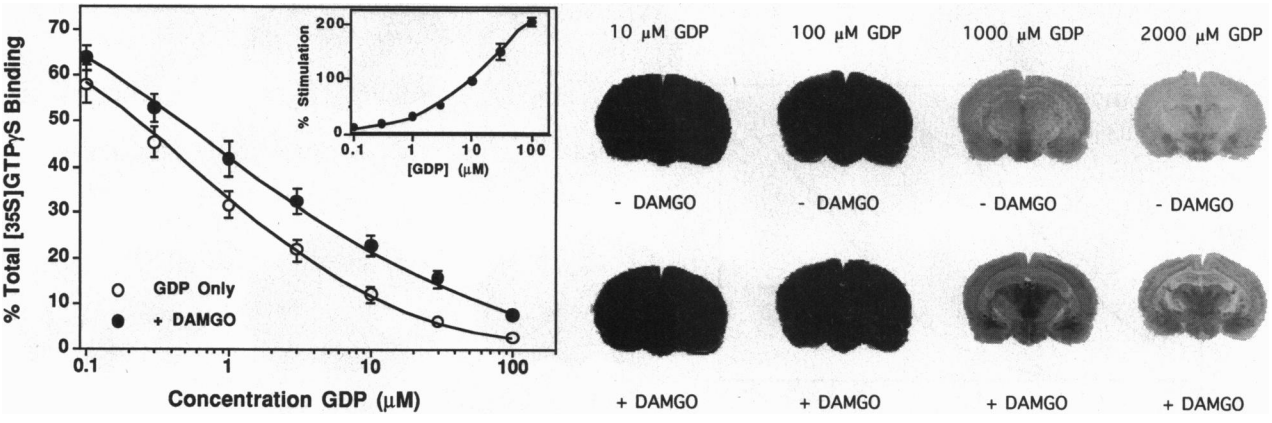

FIG. 1. Effect of GDP on basal and μ opioid-stimulated GTP[γ-^{35}S] binding in rat thalamic membranes and in rat brain sections. (*Left*) GDP concentration–effect curve of DAMGO-stimulated G-protein activity in thalamic membranes. Membranes were incubated with various concentrations of GDP in the presence and absence of 10 μM DAMGO. Data represent percentage total specific GTP[γ-^{35}S] binding measured in the absence of GDP or agonist. (*Inset*) DAMGO-stimulated GTP[γ-^{35}S] binding, expressed as percentage basal GTP[γ-^{35}S] binding at each concentration of GDP. (*Right*) Autoradiogram showing effect of GDP on GTP[γ-^{35}S] binding in rat brain sections cut at the level of the thalamus. Sections were incubated with 1–2000 μM GDP for 15 min and then GTP[γ-^{35}S] with 1–2000 μM GDP with and without 10 μM DAMGO for 2 hr.

effects of GDP (Fig. 1 *Right*). In the absence of GDP (data not shown), GTP[γ-^{35}S] produced dense labeling throughout the section, and addition of 1 or 100 μM GDP (Fig. 1) produced only a slight decrease in basal GTP[γ-^{35}S] binding. The basal level of labeling produced under these conditions was so high that addition of DAMGO had little visible effect. However, when sections were incubated with 1000 or 2000 μM GDP, basal labeling was diminished to the point that addition of DAMGO produced a visible increase in GTP[γ-^{35}S] binding, specifically in the medial thalamus, amygdala, hypothalamus, and striatum (Fig. 1 *Right*). This distribution of DAMGO-stimulated GTP[γ-^{35}S] binding corresponded to the μ opioid receptor distribution reported in receptor binding autoradiographic studies (17). Densitometric analysis of the thalamus was performed to compare the results of membrane binding assays with autoradiography. This analysis revealed that DAMGO increased GTP[γ-^{35}S] labeling in the medial thalamus by 332% and 403% in the presence of 1000 and 2000 μM GDP, respectively. These data were confirmed by direct determination of ^{35}S radioactivity in isolated sections by liquid scintillation spectrophotometry (data not shown). Since the absolute level of GTP[γ-^{35}S] binding decreased dramatically with increasing GDP, the optimal GDP concentration was chosen to demonstrate both a measurable level of bound GTP[γ-^{35}S] and a high percentage of stimulation by agonist. The optimal GDP concentration in tissue sections was 1–2 mM, in contrast to thalamic membranes where 10–30 μM was required for optimal stimulation by agonist.

The concentration–effect relationship of DAMGO stimulation of GTP[γ-^{35}S] binding was also compared between thalamic membranes and brain sections (Fig. 2). In thalamic membranes assayed in the presence of 30 μM GDP, DAMGO stimulated GTP[γ-^{35}S] binding in a concentration-dependent and saturable manner, producing maximal stimulation of 134% $\pm$ 5% compared to basal and an ED_{50} value of 214 $\pm$ 4 nM (Fig. 2 *Right*). Addition of 0.1 μM naloxone shifted the DAMGO concentration–effect curve to the right, in a manner consistent with that of a competitive antagonist. In functional assays, the potencies of antagonists can be determined from K_e values, which are calculated from the effect of the antagonist on agonist potencies. The estimated K_e value of 1.8 $\pm$ 0.3 nM for naloxone was in agreement with published values for naloxone acting at μ receptors (31). In tissue sections assayed in the presence of 2 mM GDP, DAMGO stimulated GTP[γ-^{35}S] binding with a similar concentration–effect relationship (Fig. 2 *Right*). Concentrations of 0.1 and 0.3 μM DAMGO produced small increases in GTP[γ-^{35}S] labeling in the medial thalamus, striatum, hypothalamus, and amygdala, while more significant labeling was stimulated by 1 μM DAMGO. Densitometric analysis showed that addition of 3 and 10 μM DAMGO produced relatively equal maximal increases (242% and 197%, respectively) in thalamic GTP[γ-^{35}S] labeling. This was similar to the concentrations at which maximal effects were observed with DAMGO in membranes (Fig. 2 *Left*).

If agonist-stimulated GTP[γ-^{35}S] labeling of brain sections reflected the true neuroanatomical distribution of receptor-coupled G-protein-coupled activity, then addition of appropriate antagonists should block labeling in those areas that are specifically stimulated by agonists. This criterion was explored in two receptor systems, the μ opioid receptor using DAMGO as the agonist and naloxone as the antagonist, and the cannabinoid receptor using WIN 55212-2 as the agonist. The recent development of SR141716A as a specific antagonist at cannabinoid receptors (32) offered an opportunity to satisfy this criterion for this receptor as well. Concentrations of agonists and antagonists were determined from membrane experiments and were chosen so that the concentration of antagonist used would completely block the stimulation produced by agonist concentrations required for $\approx$90% of maximal effect. Results (Fig. 3) are shown for horizontal brain sections assayed in the presence of 2 mM GDP for both receptor systems. In the case of the μ receptor, DAMGO (3 μM) stimulation of GTP[γ-^{35}S] binding was predominantly observed in striatum, medial thalamus, and periaqueductal gray. Addition of 0.3 μM naloxone completely blocked DAMGO stimulation in those areas and restored GTP[γ-^{35}S] labeling to that observed in the presence of 2 mM GDP alone. Similarly, addition of 1 μM WIN 55212-2 produced a high level of cannabinoid receptor-stimulated GTP[γ-^{35}S] binding in substantia nigra, which was completely reversed by 0.3 μM SR141716A (Fig. 3).

The neuroanatomical distribution of receptor-coupled activity was different for each receptor, as determined by comparing the distribution of μ (DAMGO), cannabinoid (WIN 55212-2), and $GABA_B$ (baclofen) receptor-stimulated GTP[γ-^{35}S] binding in horizontal sections (Fig. 4). The highest levels of DAMGO-stimulated GTP[γ-^{35}S] binding were identified in regions that included the caudate putamen (patches), medial thalamus, hypothalamus, amygdala, periaqueductal gray, dorsal raphe nucleus, nucleus locus coeruleus, parabrachial nu-

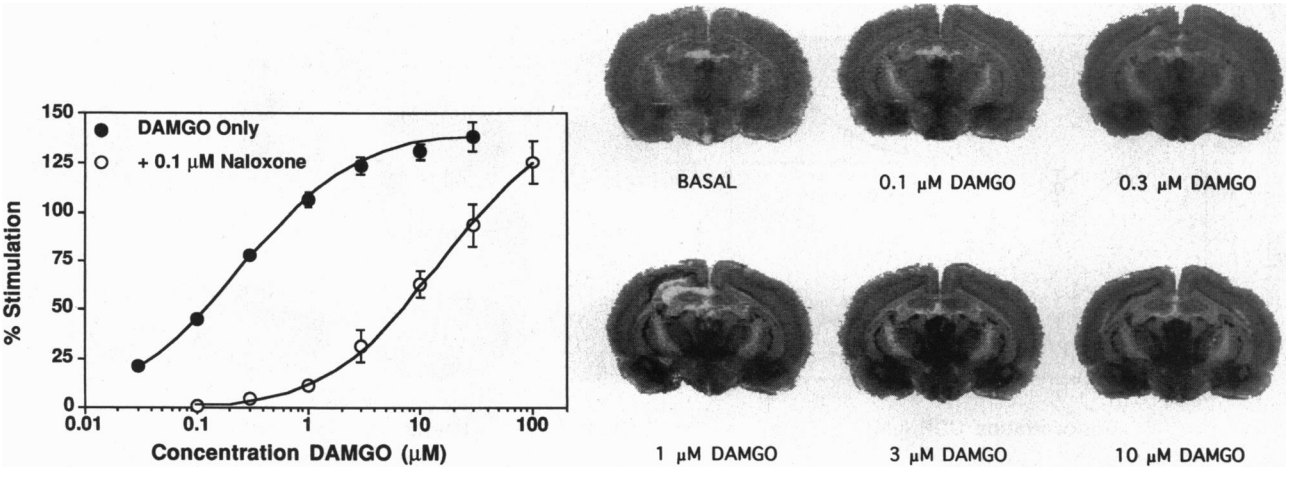

FIG. 2. Effects of various concentrations of DAMGO on μ opioid-stimulated GTP[γ-^{35}S] binding. (*Left*) GTP[γ-^{35}S] binding in thalamic membranes. Membranes were incubated with 30 μM GDP and various concentrations of DAMGO with and without 0.1 μM naloxone. Data represent percentage basal GTP[γ-^{35}S] binding measured in the presence of GDP and absence of agonist or antagonist. (*Right*) Autoradiogram of GTP[γ-^{35}S] binding in rat brain sections. Sections were incubated with 2 mM GDP for 15 min and then GTP[γ-^{35}S] with 2 mM GDP and 0.1–10 μM DAMGO for 2 hr.

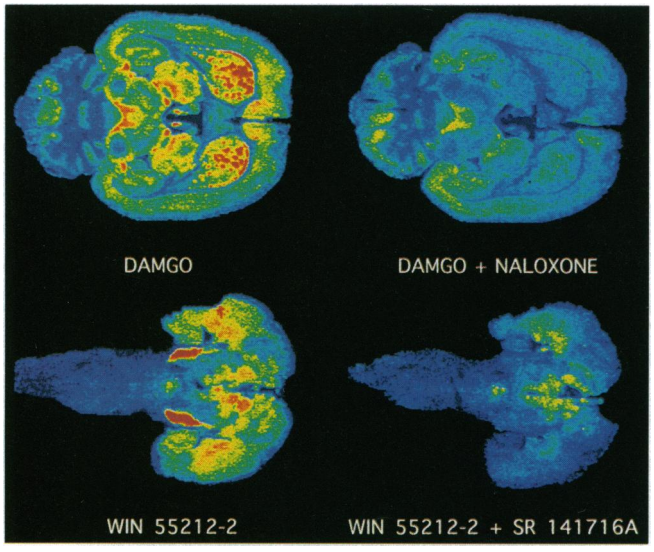

FIG. 3. Autoradiography showing antagonist reversal of agonist-stimulated GTP[γ-^{35}S] binding by μ opioid and cannabinoid receptors. Horizontal rat brain sections were cut at different levels to highlight the different areas of maximal agonist stimulation by each receptor agonist. (*Upper*) μ opioid-stimulated GTP[γ-^{35}S] binding. Sections were incubated with 2 mM GDP before adding GTP[γ-^{35}S] and 3 μM DAMGO with and without 0.3 μM naloxone. (*Lower*) Cannabinoid-stimulated GTP[γ-^{35}S] binding. Sections were incubated with 2 mM GDP for 15 min and then GTP[γ-^{35}S] with 2 mM GDP and 1 μM WIN 55212-2 with and without 0.3 μM SR141716A for 2 hr.

cleus, and nucleus tractus solitarius. WIN 55212-2-stimulated GTP[γ-^{35}S] binding was highest in the globus pallidus, caudate putamen, hippocampus, amygdala, cortex, cerebellum, and substantia nigra. Baclofen-stimulated GTP[γ-^{35}S] binding was greatest in the cortex, thalamus, superior colliculus, and cerebellum. A particularly effective comparison of GTP[γ-^{35}S] binding in response to agonists to these three receptors was seen in coronal sections at the level of the medulla (Fig. 5). In these sections, a high level of GTP[γ-^{35}S] labeling in the cerebellum was stimulated by agonists for both cannabinoid and $GABA_B$ receptors, while μ receptor-stimulated GTP[γ-^{35}S] labeling was absent in cerebellum and prominent only in the nucleus tractus solitarius.

DISCUSSION

GTP[γS] autoradiography of receptor-activated G proteins advances the study of receptor-mediated function in the central nervous system by allowing precise anatomical localization of G proteins activated in response to specific receptor agonists. The widespread applicability of the technique to various G-protein-coupled receptor systems was demonstrated in this study by examining GTP[γ-^{35}S] binding stimulated by opioid, cannabinoid, and $GABA_B$ agonists. The reliability of this technique was confirmed by showing that, for all three receptors, the qualitative neuroanatomical distribution of agonist-stimulated GTP[γ-^{35}S] binding was virtually identical to that determined by traditional receptor autoradiography (15–19). Thus, the pattern of striatal and thalamic labeling was typical for μ receptors, as was the pattern of cortical and cerebellar labeling for $GABA_B$ receptors and the pattern of striatal, hippocampal, and nigral labeling for cannabinoid receptors. The crucial difference between GTP[γ-^{35}S] autoradiography and other anatomical techniques, such as receptor autoradiography, is that GTP[γ-^{35}S] autoradiography reveals functionally active receptor populations that produce biological activity through coupling with intracellular signal transduction systems (G proteins). These results expand upon previous autoradiographic studies, which showed guanine nucleotide regulation of agonist binding (20) by providing a direct measure of receptor-activated G proteins. The functional difference between agonist and antagonist was demonstrated in Fig. 3, which showed that agonist-stimulated GTP[γ-^{35}S] binding could be specifically blocked by use of appropriate antagonists.

The critical factor in GTP[γ-^{35}S] autoradiography, as in GTP[γ-^{35}S] membrane binding assays, is the addition of excess GDP to shift the G protein into the inactive state and thus decrease basal levels of G-protein activity. It is important to note that GDP is not required for agonist stimulation but does reduce basal GTP[γ-^{35}S] binding to levels where significant agonist stimulation can be observed. Basal levels of G-protein activity must be low in order to identify receptor-stimulated

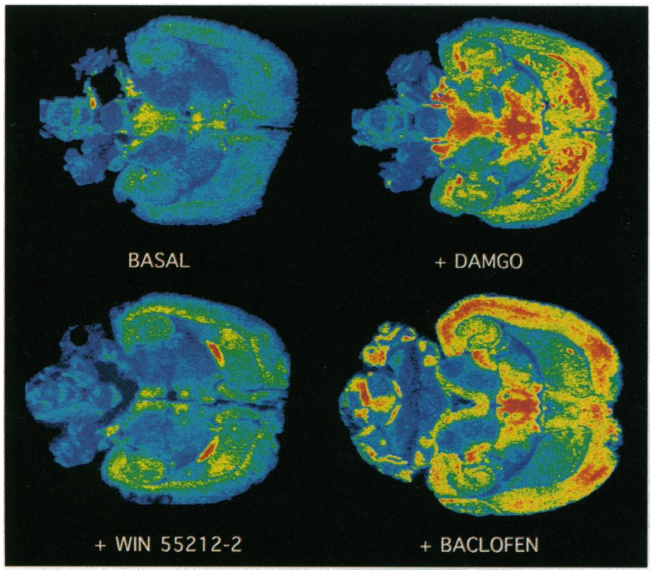

FIG. 4. Autoradiography of horizontal rat brain sections comparing distribution of GTP[γ-^{35}S] binding stimulated by μ opioid, cannabinoid, and $GABA_B$ receptors. Autoradiograms represent sections incubated with 2 mM GDP for 15 min and then GTP[γ-^{35}S] with 2 mM GDP and either DAMGO (3 μM), WIN 55212-2 (1 μM), or baclofen (300 μM) for 2 hr.

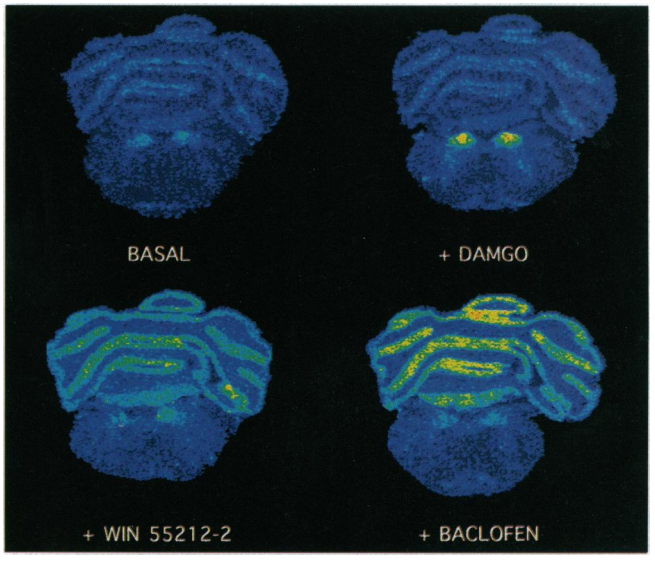

FIG. 5. Coronal sections at the level of the medulla contrasting the different distributions of agonist-stimulated GTP[γ-^{35}S] binding for μ opioid, cannabinoid, and $GABA_B$ receptors. Adjacent sections were incubated with 2 mM GDP for 15 min and then GTP[γ-^{35}S] with 2 mM GDP and either DAMGO (3 μM), WIN 55212-2 (1 μM), or baclofen (300 μM) for 2 hr.

activity, as shown in Fig. 1, where DAMGO-stimulated GTP[γ-^{35}S] binding in brain sections was virtually undetectable over basal at GDP concentrations of <1000 μM. It is not clear why up to 100 times more GDP is required to achieve reasonable basal levels of binding in tissue sections compared to isolated membranes. It is possible that the binding kinetics of guanine nucleotides to G proteins are different *in situ* as opposed to isolated membranes or that the ability of GDP to penetrate into the intracellular milieu in a brain section is limited. One important factor may be the general protein levels in brain sections, which are 10–20 times that used in membrane binding assays. An alternative explanation is that G-protein recruitment (i.e., catalytic activation of G proteins) by unoccupied receptors may differ between membranes and tissue sections.

Although the qualitative distribution of agonist-stimulated GTP[γ-^{35}S] binding was similar to that observed for standard receptor autoradiography, there were important differences in the relative levels of receptor-activated G proteins compared to receptor density. For instance, cannabinoid receptor autoradiographic studies have shown that the receptor density in the cortex is approximately one-half that in the hippocampus (15). However, the level of cannabinoid-stimulated G-protein activity in the cortex, as shown in GTP[γ-^{35}S] autoradiograms, was comparable to that in the hippocampus. Similarly, cannabinoid-stimulated G-protein activity was relatively lower in cerebellum than predicted from receptor autoradiography (15). These results may reflect differences in the efficiency of coupling of the receptor to G proteins in different brain regions, which would not have been predicted from radioligand binding assays. Putative differences in coupling efficiency were also seen between different receptor systems. For example, numerous studies have shown that the overall density of cannabinoid receptor binding sites in brain is at least 10 times that of opioid receptor sites (refs. 15, 17, 33, 34; and C. Konkoy and S.R.C., unpublished data). However, this difference was not conserved at the functional level, since overall DAMGO-stimulated G-protein activity was higher in many brain areas than cannabinoid-stimulated activity. This direct comparison is possible since cannabinoid and opioid assays were conducted on adjacent brain sections in the same experiment and analyzed on the same film. Such functional results may correlate better than radioligand binding data with the well-known physiological and behavioral data of the opioid and cannabinoid systems, which would not have predicted an excess of receptors mediating marijuana effects 10-fold greater than those mediating effects of morphine.

In addition to providing important information about the functional status of receptors in different areas of the brain, GTP[γ-^{35}S] autoradiography has several advantages over traditional radioligand receptor autoradiography from a technical perspective. First, since GTP[γ-^{35}S] is the radiolabeled ligand used in this technique, and unlabeled agonists are used to activate G proteins via specific receptors, GTP[γ-^{35}S] autoradiography is not limited by the availability of radiolabeled ligands. The technique is limited only by the availability of specific agonists and/or antagonists. Second, GTP[γ-^{35}S] autoradiography has a much shorter film exposure time than ^{3}H radioligand autoradiography (1–2 days compared to 4–20 weeks), since ^{35}S is a higher energy radioisotope than ^{3}H. Finally, multiple receptor analysis is easily performed by incubating sequential sections with a variety of agonists, as shown in the present study. Thus, simultaneous information regarding several receptor systems can be collected from the brain of a single experimental animal. Although GTP[γ-^{35}S] and receptor binding autoradiography measure different parameters in the receptor cascade, some aspects of the autoradiographic technique are conserved. In particular, it is critical to provide quantitative analysis of results. We have demonstrated this in the present study by calculating DAMGO stimulation of GTP[γ-^{35}S] binding using computer-assisted densitometry and reported the results as percentage stimulation. Thus, GTP[γ-^{35}S] autoradiography provides both anatomical and quantitative data regarding receptor-activated G proteins in tissue sections.

GTP[γ-^{35}S] autoradiography may also be combined with other anatomical techniques, including *in situ* hybridization, immunocytochemistry, and receptor autoradiography. With the combination of these techniques, a clear picture will emerge on the relationship between the individual components of the receptor–effector cascade. This is critical not only in anatomical mapping studies of receptor-activated G proteins but also to enhance traditional biochemical membrane assays by providing a guide to regions of interest for microdissection and assay. Thus, GTP[γ-^{35}S] autoradiography can provide a critical link between traditional anatomical studies and biochemical, behavioral, and physiological studies.

The authors thank Dr. Linda Porrino for helpful discussions. Ruoyu Xiao provided excellent technical assistance with image analysis. This research was supported in part by funds from U.S. Public Health Service Grants DA-02904, DA-06784, and DA-07246.

1. Birnbaumer, L., Abramowitz, J. & Brown, A. M. (1990) *Biochim. Biophys. Acta* **1031**, 163–224.
2. Brown, A. M. & Birnbaumer, L. (1990) *Annu. Rev. Physiol.* **52**, 197–213.
3. Hildebrandt, J. D., Sekura, R. D., Codina, J., Iyengar, R., Manclark, C. R. & Birnbaumer, L. (1983) *Nature (London)* **302**, 706–709.
4. Gilman, A. G. (1987) *Annu. Rev. Biochem.* **56**, 615–649.
5. Childers, S. R. (1991) *Life Sci.* **48**, 1991–2003.
6. Sim, L. J., Selley, D. E., Tsai, K. P. & Morris, M. (1994) *Brain Res.* **653**, 155–160.
7. Sim, L. J., Selley, D. E., Tsai, K. P. & Morris, M. (1994) *Brain Res.* **651**, 311–316.
8. Lewis, E. J., Harrington, C. A. & Chikaraishi, D. M. (1987) *Proc. Natl. Acad. Sci. USA* **84**, 3550–3554.
9. Aoki, C., Go, C. G., Wu, K. & Siekevitz, P. (1992) *Brain Res.* **596**, 189–201.
10. Asano, T., Shinohara, H., Morishita, R. & Kato, K. (1990) *J. Biochem.* **108**, 988–994.
11. Worley, P. F., Baraban, J. M., Van Dop, C., Neer, E. J. & Snyder, S. H. (1986) *Proc. Natl. Acad. Sci. USA* **83**, 4561–4565.
12. Matsuda, L. A., Bonner, T. I. & Lolait, S. J. (1993) *J. Comp. Neurol.* **327**, 535–550.
13. Thompson, R. C., Mansour, A., Akil, H. & Watson, S. J. (1993) *Neuron* **11**, 903–913.
14. Keith, D. E., Anton, B. & Evans, C. J. (1993) *Proc. West. Pharmacol. Soc.* **36**, 299–306.
15. Herkenham, M., Lynn, A. B., Johnson, M. R., Melvin, L. S., de Costa, B. R. & Rice, K. C. (1991) *J. Neurosci.* **11**, 563–583.
16. Chu, D. C. M., Albin, R. L., Young, A. B. & Penney, J. B. (1990) *Neuroscience* **34**, 341–357.
17. Herkenham, M. & Pert, C. B. (1982) *J. Neurosci.* **2**, 1129–1149.
18. Jansen, E. M., Haycock, D. A., Ward, S. J. & Seybold, V. S. (1992) *Brain Res.* **575**, 93–102.
19. Goodman, R. R., Snyder, S. H., Kuhar, M. J. & Young W. S., III (1980) *Proc. Natl. Acad. Sci. USA* **77**, 6239–6243.
20. Zarbin, M. A., Palacios, J. M., Wamsley, J. K. & Kuhar, M. J. (1983) *Mol. Pharmacol.* **24**, 341–348.
21. Nijssen, P. C., Sexton, T. & Childers, S. R. (1992) *J. Neurochem.* **59**, 2251–2262.
22. Herkenham, M. (1987) *Neuroscience* **23**, 1–38.
23. Asano, T., Pedersen, S. E., Scott, C. W. & Ross, E. M. (1984) *Biochemistry* **23**, 5460–5467.
24. Florio, V. A. & Sternweis, P. C. (1989) *J. Biol. Chem.* **264**, 3909–3915.
25. Traynor, J. F. & Nahorski, S. R. (1995) *Mol. Pharmacol.* **47**, 848–854.
26. Lorenzen, A., Fuss, M., Vogt, H. & Schwabe, U. (1993) *Mol. Pharmacol.* **44**, 115–123.
27. Chen, Y., Mestek, A., Liu, J., Hurley, J. A. & Yu, L. (1993) *Mol. Pharmacol.* **44**, 8–12.
28. Matsuda, L. A., Lolait, S. J., Brownstein, M. J., Young, A. L. & Bonner, T. I. (1990) *Nature (London)* **346**, 561–564.
29. Wojcik, W. J. & Neff, N. H. (1984) *Mol. Pharmacol.* **25**, 24–28.
30. Bradford, M. M. (1976) *Anal. Biochem.* **72**, 248–254.
31. Corbett, A. D., Gillan, M. G. C., Kosterlitz, H. W. & Paterson, S. J. (1985) *Br. J. Pharmacol.* **86**, 704P.
32. Rinaldi-Carmona, M., Barth, F., Heaulme, M., Shire, D., Calandra, B., Congy, C., Martinez, S., Maruani, J., Neliat, G., Caput, D., Ferrara, P., Soubrie, P., Breliere, J. C. & Le Fur, G. (1994) *FEBS Lett.* **350**, 240–244.
33. Devane, W. A., Dysarz, F. A. I., Johnson, M. R., Melvin, L. S. & Howlett, A. C. (1988) *Mol. Pharmacol.* **34**, 605–613.
34. Kuster, J., Stevenson, J., Ward, S., D'Ambra, T. & Haycock, D. (1993) *J. Pharmacol. Exp. Ther.* **264**, 1352–1363.